Homozygous DBF4 mutation as a cause for severe congenital neutropenia

Mathijs Willemsen, MD, John S. Barber, MD, Erika Van Nieuwenhove, MD, PhD, Frederik Staels, MD, PhD, Margaux Gerbaux, MD, Julika Neumann, MSc, Teresa Prezzemolo, PhD, Emanuela Pasciuto, PhD, Vasiliki Lagou, PhD, Nancy Boeckx, MD, PhD, Jessica Filtjens, PhD, Amber De Visscher, MSc, Patrick Matthys, PhD, Rik Schrijvers, MD, PhD, Thomas Tousseyn, MD, PhD, Mark O'Driscoll, PhD, Giorgia Bucciol, MD, PhD, Susan Schlenner, PhD, Isabelle Meyts, MD, PhD, Stephanie Humblet-Baron, MD, PhD, Adrian Liston, PhD

PII: S0091-6749(23)00230-0

DOI: https://doi.org/10.1016/j.jaci.2023.02.016

Reference: YMAI 15887

To appear in: *Journal of Allergy and Clinical Immunology*

Received Date: 8 September 2022

Revised Date: 23 January 2023

Accepted Date: 16 February 2023

Please cite this article as: Willemsen M, Barber JS, Van Nieuwenhove E, Staels F, Gerbaux M, Neumann J, Prezzemolo T, Pasciuto E, Lagou V, Boeckx N, Filtjens J, De Visscher A, Matthys P, Schrijvers R, Tousseyn T, O'Driscoll M, Bucciol G, Schlenner S, Meyts I, Humblet-Baron S, Liston A, Homozygous DBF4 mutation as a cause for severe congenital neutropenia, *Journal of Allergy and Clinical Immunology* (2023), doi: https://doi.org/10.1016/j.jaci.2023.02.016.

Homozygous DBF4 mutation as a cause for severe congenital neutropenia

Authors: Mathijs Willemsen, MD,[1,2*] John S. Barber, MD,[1,2*] Erika Van Nieuwenhove, MD, PhD,[1,2,3*] Frederik Staels, MD, PhD,[1,4] Margaux Gerbaux, MD,[1,5] Julika Neumann, MSc,[1,2] Teresa Prezzemolo, PhD,[1,2] Emanuela Pasciuto, PhD,[1,2] Vasiliki Lagou, PhD,[1,2] Nancy Boeckx, MD, PhD,[6] Jessica Filtjens, PhD,[7] Amber De Visscher, MSc,[7] Patrick Matthys, PhD,[7] Rik Schrijvers, MD, PhD,[4] Thomas Tousseyn, MD, PhD,[8] Mark O'Driscoll, PhD,[9] Giorgia Bucciol, MD, PhD,[10,11] Susan Schlenner, PhD,[1] Isabelle Meyts, MD, PhD,[10,11,12†] Stephanie Humblet-Baron, MD, PhD,[1†] and Adrian Liston, PhD,[1,2,13†].

Corresponding authors: Adrian Liston, al989@cam.ac.uk, phone +44 1223 496573, address Babraham Research Campus, Cambridge, CB22 3AT United Kingdom, Stephanie Humblet-Baron, stephanie.humbletbaron@kuleuven.be, phone +32 16 37 93 60, fax +32 16 33 05 91, address Herestraat 49, box 1026, 3000 Leuven, Belgium and Isabelle Meyts, isabelle.meyts@uzleuven.be, phone +32 16 34 38 41, address Herestraat 49, box 1039, 3000 Leuven, Belgium.

Affiliations:

[1] Department of Microbiology, Immunology and Transplantation, Laboratory of Adaptive Immunity, KU Leuven, Leuven, Belgium.

[2] VIB-KU Leuven Center for Brain and Disease Research, Leuven, Belgium.

[3] Department of Pediatrics, University Hospitals Leuven, Leuven, Belgium.

[4] Department of Microbiology, Immunology and Transplantation, Allergy and Clinical Immunology Research Group, KU Leuven, Leuven, Belgium.

[5] Pediatric Department, Academic Children Hospital Queen Fabiola, Université Libre de Bruxelles, Brussels, Belgium.

[6] Department of Laboratory Medicine, University Hospitals Leuven, Leuven, Belgium.

[7] Department of Microbiology, Immunology and Transplantation, Laboratory of Immunobiology, Rega Institute for Medical Research, KU Leuven, Leuven, Belgium.

[8] Department of Pathology, University Hospitals Leuven, Leuven, Belgium.

[9] Human DNA Damage Response Disorders Group, Genome Damage and Stability Centre, University of Sussex, Brighton, BN1 9RQ, United Kingdom.

[10] Department of Microbiology, Immunology and Transplantation, Laboratory for Inborn Errors of Immunity, KU Leuven, Leuven, Belgium.

[11] Department of Pediatrics, Division of Primary Immunodeficiencies, University Hospitals Leuven, Leuven, Belgium.

[12] ERN-RITA Core Center Member.

[13] Immunology Programme, The Babraham Institute, Babraham Research Campus, Cambridge, CB22 3AT United Kingdom.

* Equal contribution, co-first authors.

† Equal contribution, co-corresponding authors.

Text word count: 4467.

Abstract word count: 190.

Number of figures and tables: 4.

Number of supplementary figures and tables: 13.

Number of references: 83.

Funding:

This work was supported by the VIB Grand Challenges Program, Research Foundation (FWO)-Flanders (G.0A32.18N) the KU Leuven C1 program (C16/17/010), the European Union's Horizon 2020 research and innovation program under grant agreement No. 779295 (to AL), the KU Leuven BOFZAP start-up grant (to SHB) and the Biotechnology and Biological Sciences Research Council (BBSRC) through Institute Strategic Program Grant funding BBS/E/B/000C0427 and BBS/E/B/000C0428. IM and RS are FWO-Flanders senior clinical

investigator fellows. EVN, FS, JN, JF and ADV received a PhD fellowship from FWO-Flanders. IM is supported by the Jeffrey Modell Foundation and by the CSL Behring Chair in Primary Immunodeficiency in Children. IM and RS are members of the European Reference Network for Rare Immunodeficiency, Autoinflammation and Autoimmune Diseases (project ID No. 739543).

Disclosure of conflicts of interest:

IM is funded by the CSL Behring Chair in Primary Immune Deficiency in Children. The other authors have declared that no conflict of interest exists.

ABSTRACT

Background: Severe congenital neutropenia presents with recurrent infections early in life due to arrested granulopoiesis. Multiple genetic defects are known to block granulocyte differentiation, however a genetic cause remains unknown in approximately 40% of cases.

Objective: We aimed to characterize a patient with severe congenital neutropenia and syndromic features without a genetic diagnosis.

Methods: Whole exome sequencing results were validated using flow cytometry, Western blotting, co-immunoprecipitation, quantitative PCR, cell cycle and proliferation analysis of lymphocytes and fibroblasts and granulocytic differentiation of primary $CD34^+$ and HL-60 cells.

Results: We identified a homozygous missense mutation in *DBF4* in a patient with mild extra-uterine growth retardation, facial dysmorphism and severe congenital neutropenia. DBF4 is the regulatory subunit of the CDC7 kinase, together known as DBF4-dependent kinase (DDK), the complex essential for DNA replication initiation. The variant allele demonstrated impaired ability to bind CDC7, resulting in decreased DDK-mediated phosphorylation, defective S phase entry and progression and impaired differentiation of granulocytes associated with activation of the p53-p21 pathway. The introduction of WT DBF4 into patient $CD34^+$ cells rescued the promyelocyte differentiation arrest.

Conclusion: Hypomorphic DBF4 mutation causes autosomal recessive severe congenital neutropenia with syndromic features.

Key messages:

- Hypomorphic DBF4 mutation causes autosomal recessive severe congenital neutropenia with syndromic features.
- Hypomorphic DBF4 is associated with activation of the p53-p21 pathway in hematopoietic cells.

Capsule summary:

A homozygous hypomorphic mutation in *DBF4* causes severe congenital neutropenia with syndromic features associated with activation of the p53-p21 pathway in hematopoietic cells.

Keywords: DBF4, DNA replication, inborn errors of immunity, primary immunodeficiency, neutropenia, perturbed growth, facial dysmorphism, genetics, mutation.

Abbreviations:

CDC (cell division cycle), CDK (cyclin-dependent kinase), CMG (CDC45-MCM-GINS), DDK (DBF4-dependent kinase), DMSO (dimethyl sulfoxide), EdU (5-ethynyl-20-deoxyuridine), G-CSF (granulocyte-colony stimulating factor), GINS (Go-Ichi-Ni-San), MCM2-7 (minichromosome maintenance complex proteins 2 to 7), PBMCs (peripheral blood mononuclear cells), qPCR (quantitative polymerase chain reaction), TCR (T cell receptor), WT (wild-type).

INTRODUCTION

Severe congenital neutropenia is an inherited bone marrow failure syndrome characterized by persistently low peripheral neutrophil counts from birth. Patients typically present with recurrent infections and exhibit a promyelocyte differentiation arrest[1]. Severe congenital neutropenia is frequently associated with extra-hematopoietic features. The pathological mechanisms driving the granulocyte maturation arrest vary depending on the affected pathway[1], with 40% of cases still lacking a genetic causality[2].

DNA replication is essential for all dividing cells, and uses highly conserved pathways between cell types. Mutations in more than 20 DNA replication-associated genes cause monogenic disease which often present with developmental defects and perturbed growth, but also differentially impact specific tissues and cell types[3]. Mutations in thirteen DNA replication factors (*REQCL4*, *MCM4*, *POLE1*, *POLE2*, *POLA1*, *GINS1*, *POLD1*, *POLD2*, *MCM10*, *TOP2B*, *PRIM1*, *RPA1*, *GINS4*) present with a convergent phenotype of perturbed growth, facial anomalies and variable immune cell defects[4-21]. While immune defects are shared among multiple DNA replication-associated syndromes, only GINS1 and GINS4 deficiency are associated with congenital neutropenia, demonstrating a gene-specific as well as cell type-specific basis for sensitivity[3,10,21].

DNA replication origins are 'licensed' by the recruitment of two minichromosome maintenance complex proteins 2 to 7 (MCM2-7) during the G1 phase. Next, additional replication factors, e.g. the go-ichi-ni-san (GINS) complex and cell division cycle (CDC) 45, are recruited converting the licensed origin into two CDC45-MCM-GINS (CMG) helicases that are 'fired' during S phase.[22] The recruitment of replication factors to the licensed origin is regulated by two kinases, cyclin-dependent kinase (CDK) and dumbbell former 4 (DBF4)-dependent kinase (DDK).[23,24] DDK is a complex comprised of the CDC7 kinase and its regulatory subunit DBF4. Its primary function is to phosphorylate MCM2-7[25,26], allowing the recruitment of other

replication factors[23,24,27,28] and release of helicase activity.[29] Additional, incompletely understood, roles for the DDK in S phase checkpoint signaling, translesion DNA synthesis and replication fork metabolism have recently emerged.[30]

DDK is essential for DNA replication initiation in all organisms studied[31-34], and is regulated by periodic degradation of DBF4 outside of late G1/S phase[35-37]. DBF4 is a rate-limiting DNA replication factor in *S. cerevisiae*[38]. CDC7 and DBF4 knockout mice are early embryonic lethal, and inactivation of CDC7 or DBF4 in murine embryonic stem cells arrests DNA synthesis and causes cell death[39-41]. Partial defects in DDK may, however, be tolerated, as p53-deficiency delays embryonic lethality of CDC7 knockout[39], and CDK may compensate for its role in some contexts[42]. Here we identify a patient harboring homozygous hypomorphic *DBF4* mutation with severe congenital neutropenia and syndromic features. The hypomorphic DBF4 variant exhibits impaired CDC7-binding and DDK-mediated phosphorylation, resulting in delayed S phase entry and progression. The association of these hypomorphic effects with defective granulocyte maturation demonstrates the cell type-specific sensitivity of granulocyte progenitors to DBF4 hypomorphism.

METHODS

Study approval

Written informed consent was obtained from the patient, his relatives and all healthy controls. The UZ/KU Leuven ethics committee approved this study (S52653).

Genetic analysis

Whole exome sequencing, analysis and Sanger sequencing were performed as previously described[43,44]. For further details, see the Methods section in this article's Online Repository.

Co-immunoprecipitation

HEK293T cells were transfected with plasmids encoding FLAG-tagged wild-type (WT) or mutant DBF4 using the Lipofectamine 3000 kit (Invitrogen, Waltham, MA). After 48 hours, cells were lysed in lysis buffer (50 mM Tris-HCl (pH 7.5), 150 mM NaCl, 1.5 mM $MgCl_2$, 1% triton-X, 10% glycerol) supplemented with 1x Pierce protease inhibitors (Thermo Scientific, Waltham, MA) and 1x PhosSTOP (Roche, Basel, Switzerland). Protein concentration was quantified by Bradford Protein Assay (Bio-Rad, Hercules, CA). Precleared lysate was incubated overnight with anti-FLAG antibody (F7425, Merck Millipore, Burlington, MA) at 4°C. The antibody-protein complex was used to resuspend Dynabeads Protein G (Invitrogen) and incubated at 4°C for 1 hour, washed and resuspended in 2x NuPAGE LDS Sample buffer (Invitrogen) and 100 mM dithiothreitol. For quantification, the IP CDC7 band was normalized to the IP FLAG band.

Western blot

Western blotting was performed as previously described[44,45]. For further details, see the Methods section in this article's Online Repository.

T cell cell cycle, proliferation, phospho-flow and apoptosis assay

For details on the procedures used in experiments with stimulated T cells, see the Methods section in this article's Online Repository.

Quantitative PCR

Total RNA isolation and qPCR was performed as previously described[44]. For further details, see the Methods section in this article's Online Repository.

Fibroblast growth curve and serum starvation assay

Exponentially-growing fibroblasts were seeded in a 6-well plate in 3 ml of complete DMEM and harvested at the indicated time points. Total cell numbers and viability were assessed with trypan blue (Gibco) exclusion using a TC20 Automated Cell Counter (Bio-Rad).

Exponentially-growing fibroblasts were plated in 6-well plates and serum starved in DMEM (Gibco) supplemented with 10 mM HEPES (Gibco) and 0.5% FBS (Tico Europe, Amstelveen, the Netherlands) for 72 hours. After synchronization, cells were released in DMEM (Gibco) supplemented with 10 mM HEPES (Gibco), 1x MEM Non-Essential Amino Acids Solution (Gibco) and 20% FBS (Tico Europe) for the indicated duration. One hour before harvest 10 µM EdU was added. Cells were collected, washed and stained with Fixable Viability Dye eFluor 780 (Invitrogen). Fibroblasts were fixed using the Foxp3 Transcription Factor Fixation kit (Invitrogen) and EdU visualized using the Click-iT EdU Pacific Blue Flow Cytometry Assay Kit (Invitrogen). DNA was stained using FxCycle PI/RNase Staining Solution (Invitrogen). Cells were acquired on a BD FACSCanto II and analyzed using FlowJo software.

Fibroblasts single cell cycle progression assay

Exponentially growing fibroblasts were seeded, serum-starved and released as described above with the addition of 20 µM EdU (Invitrogen), 100 ng/ml nocodazole (Sigma-Aldrich, Saint Louis, MO) with or without TAK-931 (MedChemExpress, NJ) to the release medium. Fibroblasts were stained, acquired and analyzed as described above.

209 **HL60 cells differentiation**

210 HL60 cells were differentiated to granulocyte-like cells as previously described[44]. For further
211 details, see the Methods section in this article's Online Repository.

212

213 **Lentivirus production**

214 Lentivirus was produced as previously described[46]. For further details, see the Methods section
215 in this article's Online Repository.

216

217 **CD34$^+$ cell isolation, transduction and granulocytic differentiation**

218 Isolation, transduction and granulocytic differentiation of CD34$^+$ cells were performed as
219 previously described[44,47]. For further details, see the Methods section in this article's Online
220 Repository.

221

222 **Statistics**

223 The mean of groups was compared using an unpaired T test or ordinary one-way ANOVA with
224 Tukey's multiple comparisons test when appropriate. A p-value <0.05 was considered
225 significant. Statistics was performed using GraphPad Prism 9.3.1.

226

RESULTS

Homozygous hypomorphic DBF4 mutation in a patient with syndromic severe congenital neutropenia

The male proband was born at term to consanguineous parents of Turkish descent (Fig 1, *A*). His birth weight was 3090 g (-0.9 SD). From 2 months of age, he repeatedly presented with otitis media, once complicated by mastoiditis, and oral candidiasis, requiring three hospital admissions by age 1 year. Fever, high inflammatory parameters, and poor neutrophilic response were noted. At presentation in our tertiary reference center, complete blood count showed leukopenia with complete agranulocytosis and absolute lymphopenia (see Table E1 in the Online Repository). Lymphocytes proliferated in response to mitogens, and had a low response to recall antigens (see Table E2 in the Online Repository). Bone marrow biopsy revealed a promyelocyte differentiation arrest compatible with severe congenital neutropenia (Fig 1, *B*; see Table E1 in the Online Repository). Daily subcutaneous injections of 7.5 µg/kg granulocyte-colony stimulating factor were initiated which normalized the patient's neutrophil counts (Fig 1, *C*; see Table E1 and Fig E1 in the Online Repository).

Until age 7 years the patient had transient anemia, with suboptimal nutritional status, and transient relative lymphopenia (see Fig E1 in the Online Repository). During infectious episodes leukopenia, including absolute neutropenia, and absolute lymphopenia would recur (Fig 1, *C*; see Fig E1 in the Online Repository). Chronic hypergammaglobulinemia was also noted (see Fig E1 in the Online Repository). Despite normal granulocyte counts, multiple treatment escalations and/or hospitalizations were required for infections (Fig 1, *C*; see Fig E1 in the Online Repository). Chest-computed tomography obtained at age 7 years showed bronchiectasis, which spurred initiation of antibiotic prophylaxis with cefuroxime-axetil and daily positive expiratory pressure mask physiotherapy. Azithromycin maintenance (3 x 10 mg/kg weekly) was initiated at age 8.5 years, significantly reducing the frequency of infections (see Fig E1 in the Online Repository). Flow cytometry performed between the age of 9 to 21

years revealed non-specific signs of T cell dysfunction with normal numbers of T, B and NK cells (see Table E3 in the Online Repository). A chromosome fragility assay performed at age 18 years was unrevealing (see Table E2 in the Online Repository). Additionally, both mild facial dysmorphism (synophrys, prominent nasal bridge and pointed chin) and growth retardation, partially responsive to enteral feeding support, were observed. The patient is now a young adult, with height -1.0 SD and weight -2.8 SD (see Fig E2 in the Online Repository). He suffers from mild intellectual disability (WISC-III IQ 50 at age 10 years) and is in adapted schooling.

Clinical genetic testing at the time of presentation revealed no pathogenic mutation in *ELANE*, *HAX1* and *G6PC3*. We then performed family whole-exome sequencing, with 33 homozygous, 3 compound heterozygous and 42 *de novo* variants (see Table E4-E6 in the Online Repository), of which the lead was a homozygous mutation in *DBF4* (c.627A>C, p.K209N). The variant allele and its segregation with disease were confirmed by Sanger sequencing (Fig 1, *A* and *D*). The c.627A>C *DBF4* variant is reported only once in heterozygous state (allele frequency 4.01×10^{-6}) in the gnomAD v2.1.1 database, affects a conserved residue (Fig 1, *E*), is predicted deleterious by *in silico* tools (SIFT: 0.05, PolyPhen-2: 0.991, CADD score: 25.8 with a *DBF4*-specific mutation significance cutoff of 3.13)[48-51], and is rarer and has a higher CADD score than homozygous variants reported in gnomAD v2.1.1 (Fig 1, *F*). These features identified the DBF4 variant as the key candidate for further investigation.

The DBF4 protein harbors three conserved motifs: N, middle (M) and C. Motif N is responsible for DDK docking on MCM2, while motifs M and C enable CDC7 binding and activation (Fig 1, *G*)[25,52]. As residue K209 is located in close proximity to motif M, we investigated potential effects of K209N on CDC7 binding. We performed co-immunoprecipitation assays using FLAG-tagged DBF4 alleles in HEK293T cells. Overexpression efficiency of FLAG-tagged WT and variant DBF4 was similar, indicating normal protein stability (Fig 1, *H*). Co-immunoprecipitation showed that the K209N variant significantly reduced CDC7-binding capacity, compared to the WT allele (Fig 1, *H* and *I*). This effect does not exclude additional

potential detrimental effects of the K209N substitution, with motif M also being demonstrated to contribute to CDC7 kinase activity[53] and the analogous residue participating in MCM4-binding in *S. cerevisiae*[26]. Together, we identified a rare homozygous DBF4 variant hypomorphic for CDC7 binding in a patient with syndromic severe congenital neutropenia.

The K209N DBF4 variant is associated with a functional impact on S phase entry

We utilized patient T cells, an intact primary cell population, to evaluate the functional consequences of reduced DDK formation. We stimulated PBMCs with anti-CD3 and anti-CD28 and discriminated cell cycle stages by flow cytometry (Fig 2, *A*). Following stimulation, a cell cycle defect in patient T cells was observed, with a persistent decrease in the percentage of cells entering S phase compared to healthy controls (Fig 2, *A* and *B*; see Fig E3 in the Online Repository). This defective entry translated into impaired proliferation of patient cells (Fig 2, *C* and *D*). The cell cycle and proliferation defects occurred distal from T cell receptor (TCR) signaling, as evident by normal phosphorylation of extracellular signal-regulated kinase and upregulation of activation markers CD25 and HLA-DR (see Fig E3 in the Online Repository). Together, this demonstrates that patient T cells have an S phase entry and proliferation defect upon stimulation, despite intact TCR signaling.

At the molecular level, DBF4 gene and protein expression were similar in stimulated T cells from the patient and healthy controls. Phosphorylation of MCM2 at two DDK-dependent residues was intact, albeit associated with increased CDC7 protein expression in patient T cells (Fig 2, *E*; see Fig E4 in the Online Repository). We found gene and protein expression of CDK inhibitor *CDKN1A* (encoding p21) to be increased in stimulated patient T cells (Fig 2, *E*; see Fig E4 in the Online Repository), potentially related to the cell cycle and proliferation defect as p21 can mediate a G1 arrest[54,55]. p21 upregulation seemed to be driven by altered p53 protein dynamics, as p53 protein but not gene expression was increased (Fig 2, *E*; see Fig E4 in the Online Repository). Markers for DNA-damage, such as S15-p53 and S139-H2AX phosphorylation[56,57], and DNA replication stress, such as S8-RPA32/2 and S317-CHK1

phosphorylation[58,59], were not elevated in patient cells, arguing against this being the source of p53 stabilization (Fig 2, *E*; see Fig E4 in the Online Repository). The G1 arrest combined with activation of the p53-p21 pathway is reminiscent of activation of the p53-dependent DNA replication origin activation checkpoint[60-62]. This checkpoint functions to ensure that replicating cells only enter S phase when sufficient DNA replication origins are licensed. When insufficient origins are licensed, the Forkhead transcription factor FOXO3 activates the p14-Mouse double minute 2 homolog (MDM2)-p53-p21/Dickkopf homolog 3 (DKK3) pathway which arrests cells in G1[62]. Although gene expression of *FOXO3* was comparable between stimulated T cells from the patient and healthy controls, gene expression of *CDKN2A* (encoding p14), which is known to stabilize the p53 protein by degrading its negative regulator MDM2[63,64], and Wnt/β-catenin signaling antagonist *DKK3* were significantly increased, raising the possibility of (partial) activation of the DNA replication origin activation checkpoint in stimulated patient T cells (see Fig E4 in the Online Repository). Increased p53 protein expression can not only result in cell cycle arrest, but also in apoptosis. We observed a significantly increased percentage of early apoptotic cells in stimulated T cells, especially $CD8^+$ T cells, from the patient compared to healthy controls, and a trend towards increased gene expression of *PMAIP1*, a pro-apoptotic p53 target gene (Fig 2, *F* and *G*; see Fig E4 in the Online Repository). Together, these data suggest that the cell cycle and proliferation defects observed in patient T cells are mediated by activation of the p53-p21 pathway.

Next, to study the role of DBF4 in the observed proliferative defects, we used primary dermal fibroblasts. Patient fibroblasts grew at a similar rate as healthy controls (see Fig E5 in the Online Repository). Nevertheless, patient exponentially-growing fibroblasts showed increased expression of total MCM2, accompanied by a proportional increase in S40/41-MCM2 phosphorylation and a 40-50% reduction in S139-MCM2 phosphorylation when normalized to total MCM2 (Fig 3, *A*; see Fig E5 in the Online Repository). Similar to stimulated T cells, CDC7 protein expression was increased (Fig 3, *A*; see Fig E5 in the Online Repository). We did not observe activation of the p53-p21 pathway in patient fibroblasts, p21 protein expression was

even significantly decreased (Fig 3, *A*; see Fig E5 in the Online Repository). The reduction in DDK activity in patient fibroblasts was accompanied by defective entry into S phase. Using synchronization in G0 by serum starvation, and release by serum addition, we observed a persistent decrease in the percentage of cells entering S phase compared to healthy controls (Fig 3, *B* and *C*; see Fig E5 in the Online Repository). We also noted a slower accumulation of patient fibroblasts in G2/M, suggesting that patient fibroblasts have an S phase entry and progression defect (Fig 3, *B* and *C*; see Fig E5 in the Online Repository). By releasing synchronized fibroblasts into medium containing EdU and nocodazole, which halts cells in mitosis, we could monitor progression through a single cell cycle. Using this system, again fewer patient fibroblasts entered the cell cycle at an early time-point with entry substantially delayed, and more patient fibroblasts had sub-G1 DNA content at a later time-point (Fig 3, *D* and *E*; see Fig E6 in the Online Repository). The only known function of DBF4 is to regulate CDC7 kinase activity[30], therefore given the lower CDC7 binding capacity of the DBF4 variant allele, the cell cycle defects in both stimulated T cells and serum-starved fibroblasts and the decrease in S139-MCM2 phosphorylation in unchallenged fibroblasts we reasoned that the DBF4 variant allele must be hypomorphic for cell cycle progression. If so, additional DDK inhibition should induce a more prominent phenotype in patient fibroblasts. The single cell cycle progression assay allowed us to test the role of DDK function in the patient phenotype, using the most specific DDK inhibitor described thus far, TAK-931[65]. Following synchronization, we observed a relative reduction in G2/M patient fibroblasts upon treatment with TAK-931 compared to healthy controls, consistent with an elevated sensitivity towards DDK inhibition for S-G2/M progression (Fig 3, *D* and *F*; see Fig E6 in the Online Repository). The increased sensitivity was associated with an increased percentage of patient fibroblasts in S phase, indicating that the patient fibroblasts with delayed S phase entry also show delayed S phase progression upon DDK inhibition (Fig 3, *D* and *G*). Together, these data reveal that the defect in S phase entry, progression and S139-MCM2 phosphorylation is coupled with an increased sensitivity to DDK inhibition, providing evidence that the DBF4 variant allele is hypomorphic for cell cycle progression.

Promyelocyte differentiation arrest is rescued by WT DBF4 expression and associated with p53-p21 pathway activation

To investigate the necessity for DDK activity during granulocytic differentiation, we turned to the human promyelocytic leukemia cell line HL60. HL60 cells differentiate into neutrophil-like cells upon exposure to dimethyl sulfoxide (DMSO). After 6 days of differentiation in the presence of TAK-931, we observed an accumulation of promyelocytic cells with a decrease in the percentage of neutrophil-like cells (Fig 4, *A* and *B*). Significant cell death occurred with increasing concentrations of TAK-931 (see Fig E7 in the Online Repository), potentially related to the $p53^{null}$ status of HL60 cells[60]. Nevertheless, cell death after 6 days of differentiation occurred predominantly in differentiating $CD11b^{+}$ cells (see Fig E7 in the Online Repository). Thus, in this *in vitro* model of human granulopoiesis, DDK activity seems to be necessary for human granulocytic differentiation.

Having established a link between human granulopoiesis and DDK activity, we sought to recapitulate the patient's neutropenia phenotype *in vitro*. Peripheral blood $CD34^{+}$ cells from the patient and two healthy controls were differentiated into granulocytes through *in vitro* culture. Morphologic assessment and flow cytometry showed a granulocyte differentiation arrest at the promyelocyte stage in patient cells, recapitulating the *in vivo* findings (Fig 4, *C* and *D*, see Fig E7 in the Online Repository). This phenotype was associated with increased *CDKN1A* gene expression in patient-derived cells after 16 days of differentiation (Fig 4, *E*). Both *CDKN1A* gene expression and p53 protein expression were increased in *ex vivo* granulocytes (Fig 4, *E* and *F*). We also observed a slightly increased percentage of early apoptotic myelocytes among patient cells compared to healthy controls (see Fig E7 in the Online Repository). The activation of the p53-p21 pathway and increased apoptosis rate in patient granulocytic cells agree with our findings in stimulated T cells and differentiating HL60 cells treated with TAK-931, and suggest that differentiating granulocytes past the promyelocyte stage are particularly sensitive to decreased DDK activity. Finally, to establish a causal relationship between the promyelocyte differentiation arrest and the DBF4 variant allele, we

introduced WT DBF4 into patient CD34$^+$ cells through lentiviral transduction. WT DBF4 expression, but not GFP expression, normalized the percentage of promyelocytes and myelocytes and slightly increased the percentage of metamyelocytes and neutrophils among patient cells after 13 days of differentiation (Fig 4, *C* and *D*), providing definitive genetic evidence for a phenotype-genotype relationship.

DISCUSSION

We report a homozygous mutation in *DBF4* associated with mild facial dysmorphism, growth retardation, mild intellectual disability and severe congenital neutropenia. This phenotype shows both significant overlap with previously reported DNA replication-associated syndromes, especially GINS1 and GINS4 deficiency[3,10,20,21], and also distinct immunological features. For example, in functional DBF4, GINS1 and GINS4 deficiency T and B cells seem to be relatively spared, while deficiencies in subunits of the replicative DNA polymerases ε and δ are associated with a combined immunodeficiency without neutropenia[7,8,10-12,14,20,21]. Furthermore, other DNA replication-associated syndromes have no immunological phenotype, providing further evidence for a gene-specific effect rather than an inevitable consequence of cell cycle defects[3,21].

The addition of functional DBF4 deficiency to GINS1 and GINS4 deficiency as a genetic cause of congenital neutropenia suggests a common class of functional effect. Typically, a promyelocyte arrest is observed in the bone marrow, suggesting a unique vulnerability during this stage of granulopoiesis[1]. With GINS1, GINS4 and functional DBF4 deficiency driving neutropenia, this suggests a specific dependency on these factors, but not other DNA replication factors with documented disorders, during the differentiation of promyelocytes to mature neutrophils, and marks a new category of congenital neutropenia: those caused by defects in DNA replication factors. A potential explanation of this new category is the high proliferation occurring at the promyelocyte/myelocyte stage of human granulopoiesis, followed

by cell cycle arrest to allow differentiation[66,67]. Accordingly, gene expression of *DBF4* and other DNA replication factors is higher in promyelocytes compared to mature neutrophils[67]. The granulocyte differentiation arrest in GINS1 deficiency is characterized by the accumulation of both promyelocytes and, unlike our patient, myelocytes in the bone marrow, and was associated with only few infections and intact emergency granulopoiesis[10]. Similarly, the GINS4-deficient patients only required intermittent G-CSF treatment[20], arguing for a more severe congenital neutropenia phenotype in the DBF4 patient. Other DNA replication-associated syndromes do not present with neutropenia, suggesting this is a gene-specific phenotype[3,21].

The increased severity of neutropenia in the DBF4 hypomorphic patient, compared to GINS1- and GINS4-deficient patients and, in particular, other DNA replication-associated syndromes, can be explained by either a quantitative or qualitative defect. While increasing severity of DNA replication impairment could result in increased cellular phenotype due to only quantitative effects, the data presented here on other leukocytes argues for a qualitative difference. While the neutropenia in functional DBF4 deficiency is more severe, the opposite is true for the growth and NK cell phenotype. In contrast to our patient, GINS1-deficient patients suffer from severe intra-uterine growth retardation and near complete NK lymphopenia.[10] Likewise, decreased fibroblast proliferation was only observed in GINS1-deficient patients.[10] These differences suggest that the various clinical manifestations of DNA replication-associated syndromes are driven by differential sensitivity of certain cell types to deficiencies in specific DNA replication factors. Alternatively, these differences might reflect non-redundant roles of DNA replication factors in specific cell types unrelated to DNA replication.

A potential explanation for the qualitative model of cellular manifestations of DNA replication-associated syndromes is the biochemical impact of deficiency. In contrast to GINS1 deficiency, both functional DBF4- and GINS4-deficient cells did not show evidence of increased DNA damage, arguing that this is not a prerequisite for the neutropenia phenotype[10,20]. Our experiments indicate that the DBF4 K209N variant has lower CDC7 binding capacity than the

WT protein, but we found evidence of lower MCM2 DDK-specific phosphorylation only at S139, and not at S40/41, in unchallenged fibroblasts. Although both DDK-dependent S40/41 and S139 MCM2 phosphorylation are essential for DNA replication initiation in human cells[68], it was recently shown that the threshold of S139-MCM2 phosphorylation, but not S40/41-MCM2 phosphorylation, necessary to activate baseline versus dormant DNA replication origins is higher for the latter[69]. These data provide a possible explanation why we only observe a defect in S139-MCM2 phosphorylation in unchallenged patient fibroblasts, and could indicate defective dormant origin activation. Despite cell cycle and proliferation defects, we were unable to detect a DDK-dependent MCM2 phosphorylation defect in stimulated T cells. The differences observed between fibroblasts and T cells argue in favor of cell type-specific effects of functional DBF4 deficiency and/or differential regulation of MCM2 post-translational modifications. Nevertheless, in contrast to fibroblasts, we found that DBF4 hypomorphic hematopoietic cells (i.e. stimulated T cells, *ex vivo* granulocytes and differentiating $CD34^+$ cells) inappropriately activated the p53-p21 pathway. p53-p21 serves to stall cell cycle progression and induce apoptosis, processes that might disproportionally affect granulopoiesis. This hypothesis is supported by the finding of p53-p21 pathway activation in patient hematopoietic cells as this pathway is implicated in several bone marrow failure syndromes, including 5q- syndrome, Diamond-Blackfan anemia, Fanconi anemia, Shwachman-Diamond(-like) syndromes and dyskeratosis congenita[70-75]. Direct evidence of p53-p21 pathway involvement in bone marrow failure comes from germline gain-of-function mutations in *TP53* and loss-of-function mutations in *MDM4*, a negative regulator of p53, which cause bone marrow failure syndromes with enhanced p53 transcriptional activity[76,77]. These data implicate activation of the p53-p21 pathway as the molecular basis for the cell type-specific effect of DBF4 hypomorphism on neutrophil precursors.

How functional DBF4 deficiency causes p53-p21 pathway activation remains an open question. Our data from stimulated T cells seem to exclude DNA damage and replication stress as culprits. Activation of the DNA replication origin activation checkpoint seems plausible as CDC7 knockdown and pharmacological DDK inhibition activate this checkpoint in

untransformed dermal fibroblasts[60-62]. We found increased gene and/or protein expression of nearly all components of this pathway in stimulated patient T cells, except for the initiating Forkhead transcription factor FOXO3. It is, however, noteworthy to mention that the activity of FOXO transcription factors is primary regulated by changes in their subcellular localization[78]. Additionally, the cellular models used to elucidate the molecular architecture of this checkpoint employed near-complete CDC7 knockdown or pharmacological DDK inhibition, potentially allowing room for intermediate phenotypes to arise in conditions with residual DDK activity. We did not observe activation of this checkpoint in exponentially-growing patient fibroblasts, suggesting that sufficient residual DDK activity remains for fibroblasts to proliferate normally. This is also supported by the lack of a growth deficit in patient fibroblasts.

Activation of the p53-p21 pathway is also interesting from a therapeutic standpoint, as it might be related to G-CSF efficacy. G-CSF induces granulopoiesis through upregulation of nicotinamide adenine dinucleotide (NAD)-dependent sirtuin-1, which is subsequently able to activate emergency granulopoeisis[79]. Sirtuin-1 is a deacetylase with the ability to target p53 and attenuate its transcriptional activity[80]. Accordingly, G-CSF treatment suppressed *CDKN1A* gene expression in primary myeloid bone marrow cells from healthy controls[81] and inhibition of NAD production resulted in p53 activation, p21 upregulation and diminished granulocytic differentiation of human induced pluripotent stem cells[82]. Additionally, administration of vitamin B3 (nicotinamide, precursor of NAD) resulted in increased peripheral granulocyte count in healthy controls[79] and improved response to G-CSF in severe congenital neutropenia patients[83]. Altogether, these data suggest that the activation status of the p53-p21 pathway might be related to the efficacy of G-CSF treatment in congenital neutropenia patients.

In conclusion, we report a novel DNA replication-associated inborn error of immunity characterized by syndromic severe congenital neutropenia as a result of a homozygous hypomorphic *DBF4* mutation. Our findings add *DBF4* to the list of genetic causes of severe congenital neutropenia and implicate inappropriate activation of the p53-p21 pathway in its pathogenesis. This report also adds to the growing literature suggesting that mutations in DNA

507 replication factors can lead to convergent phenotypes of perturbed growth, facial anomalies
508 and diverse immune cell defects[21].

509

510 **ACKNOWLEDGEMENTS**

511

512 The authors would like to thank the patient and his family for participating in this study. The
513 authors would also like to thank Leen Moens for logistical support and the KU Leuven Flow
514 and Mass Cytometry Facility for technical assistance.

515

516 **REFERENCES**

517

518 1. Skokowa J, Dale DC, Touw IP, Zeidler C, Welte K. Severe congenital neutropenias. Nat
519 Rev Dis Primers 2017; 3:17032.

520 2. Donadieu J, Beaupain B, Fenneteau O, Bellanne-Chantelot C. Congenital neutropenia in
521 the era of genomics: classification, diagnosis, and natural history. Br J Haematol 2017;
522 179:557-74.

523 3. Bellelli R, Boulton SJ. Spotlight on the Replisome: Aetiology of DNA Replication-
524 Associated Genetic Diseases. Trends Genet 2021; 37:317-36.

525 4. Kitao S, Shimamoto A, Goto M, Miller RW, Smithson WA, Lindor NM, et al. Mutations in
526 RECQL4 cause a subset of cases of Rothmund-Thomson syndrome. Nat Genet 1999;
527 22:82-4.

528 5. Hughes CR, Guasti L, Meimaridou E, Chuang CH, Schimenti JC, King PJ, et al. MCM4
529 mutation causes adrenal failure, short stature, and natural killer cell deficiency in humans.
530 J Clin Invest 2012; 122:814-20.

531 6. Gineau L, Cognet C, Kara N, Lach FP, Dunne J, Veturi U, et al. Partial MCM4 deficiency
532 in patients with growth retardation, adrenal insufficiency, and natural killer cell deficiency.
533 J Clin Invest 2012; 122:821-32.

534 7. Pachlopnik Schmid J, Lemoine R, Nehme N, Cormier-Daire V, Revy P, Debeurme F, et al.
535 Polymerase epsilon1 mutation in a human syndrome with facial dysmorphism,
536 immunodeficiency, livedo, and short stature ("FILS syndrome"). J Exp Med 2012;
537 209:2323-30.

8. Frugoni F, Dobbs K, Felgentreff K, Aldhekri H, Al Saud BK, Arnaout R, et al. A novel mutation in the POLE2 gene causing combined immunodeficiency. J Allergy Clin Immunol 2016; 137:635-8.e1.

9. Starokadomskyy P, Gemelli T, Rios JJ, Xing C, Wang RC, Li H, et al. DNA polymerase-alpha regulates the activation of type I interferons through cytosolic RNA:DNA synthesis. Nat Immunol 2016; 17:495-504.

10. Cottineau J, Kottemann MC, Lach FP, Kang YH, Vely F, Deenick EK, et al. Inherited GINS1 deficiency underlies growth retardation along with neutropenia and NK cell deficiency. J Clin Invest 2017; 127:1991-2006.

11. Logan CV, Murray JE, Parry DA, Robertson A, Bellelli R, Tarnauskaite Z, et al. DNA Polymerase Epsilon Deficiency Causes IMAGe Syndrome with Variable Immunodeficiency. Am J Hum Genet 2018; 103:1038-44.

12. Conde CD, Petronczki OY, Baris S, Willmann KL, Girardi E, Salzer E, et al. Polymerase delta deficiency causes syndromic immunodeficiency with replicative stress. J Clin Invest 2019; 129:4194-206.

13. Mace EM, Paust S, Conte MI, Baxley RM, Schmit MM, Patil SL, et al. Human NK cell deficiency as a result of biallelic mutations in MCM10. J Clin Invest 2020; 130:5272-86.

14. Cui Y, Keles S, Charbonnier LM, Jule AM, Henderson L, Celik SC, et al. Combined immunodeficiency caused by a loss-of-function mutation in DNA polymerase delta 1. J Allergy Clin Immunol 2020; 145:391-401.e8.

15. Parry DA, Tamayo-Orrego L, Carroll P, Marsh JA, Greene P, Murina O, et al. PRIM1 deficiency causes a distinctive primordial dwarfism syndrome. Genes Dev 2020; 34:1520-33.

16. Van Esch H, Colnaghi R, Freson K, Starokadomskyy P, Zankl A, Backx L, et al. Defective DNA Polymerase alpha-Primase Leads to X-Linked Intellectual Disability Associated with Severe Growth Retardation, Microcephaly, and Hypogonadism. Am J Hum Genet 2019; 104:957-67.

17. Broderick L, Yost S, Li D, McGeough MD, Booshehri LM, Guaderrama M, et al. Mutations in topoisomerase IIβ result in a B cell immunodeficiency. Nat Commun 2019; 10:3644.

18. Papapietro O, Chandra A, Eletto D, Inglott S, Plagnol V, Curtis J, et al. Topoisomerase 2β mutation impairs early B-cell development. Blood 2020; 135:1497-501.

19. Sharma R, Sahoo SS, Honda M, Granger SL, Goodings C, Sanchez L, et al. Gain-of-function mutations in RPA1 cause a syndrome with short telomeres and somatic genetic rescue. Blood 2022; 139:1039-51.

20. Conte MI, Poli MC, Taglialatela A, Leuzzi G, Chinn IK, Salinas SA, et al. Partial loss-of-function mutations in GINS4 lead to NK cell deficiency with neutropenia. JCI Insight 2022; 7.

21. Willemsen M, Staels F, Gerbaux M, Neumann J, Schrijvers R, Meyts I, et al. DNA replication-associated inborn errors of immunity. J Allergy Clin Immunol 2022.

22. Fragkos M, Ganier O, Coulombe P, Mechali M. DNA replication origin activation in space and time. Nat Rev Mol Cell Biol 2015; 16:360-74.

23. Heller RC, Kang S, Lam WM, Chen S, Chan CS, Bell SP. Eukaryotic origin-dependent DNA replication in vitro reveals sequential action of DDK and S-CDK kinases. Cell 2011; 146:80-91.

24. Yeeles JT, Deegan TD, Janska A, Early A, Diffley JF. Regulated eukaryotic DNA replication origin firing with purified proteins. Nature 2015; 519:431-5.

25. Greiwe JF, Miller TCR, Locke J, Martino F, Howell S, Schreiber A, et al. Structural mechanism for the selective phosphorylation of DNA-loaded MCM double hexamers by the Dbf4-dependent kinase. Nat Struct Mol Biol 2022; 29:10-20.

26. Saleh A, Noguchi Y, Aramayo R, Ivanova ME, Stevens KM, Montoya A, et al. The structural basis of Cdc7-Dbf4 kinase dependent targeting and phosphorylation of the MCM2-7 double hexamer. Nat Commun 2022; 13:2915.

27. Randell JC, Fan A, Chan C, Francis LI, Heller RC, Galani K, et al. Mec1 is one of multiple kinases that prime the Mcm2-7 helicase for phosphorylation by Cdc7. Mol Cell 2010; 40:353-63.

28. Deegan TD, Yeeles JT, Diffley JF. Phosphopeptide binding by Sld3 links Dbf4-dependent kinase to MCM replicative helicase activation. EMBO J 2016; 35:961-73.

29. Sheu YJ, Stillman B. The Dbf4-Cdc7 kinase promotes S phase by alleviating an inhibitory activity in Mcm4. Nature 2010; 463:113-7.

30. Dolson A, Sauty SM, Shaban K, Yankulov K. Dbf4-Dependent Kinase: DDK-ated to post-initiation events in DNA replication. Cell Cycle 2021; 20:2348-60.

31. Jackson AL, Pahl PM, Harrison K, Rosamond J, Sclafani RA. Cell cycle regulation of the yeast Cdc7 protein kinase by association with the Dbf4 protein. Mol Cell Biol 1993; 13:2899-908.

32. Takeda T, Ogino K, Matsui E, Cho MK, Kumagai H, Miyake T, et al. A fission yeast gene, him1(+)/dfp1(+), encoding a regulatory subunit for Hsk1 kinase, plays essential roles in S-phase initiation as well as in S-phase checkpoint control and recovery from DNA damage. Mol Cell Biol 1999; 19:5535-47.

33. Jiang W, McDonald D, Hope TJ, Hunter T. Mammalian Cdc7-Dbf4 protein kinase complex is essential for initiation of DNA replication. EMBO J 1999; 18:5703-13.

34. Jares P, Luciani MG, Blow JJ. A Xenopus Dbf4 homolog is required for Cdc7 chromatin binding and DNA replication. BMC Mol Biol 2004; 5:5.

35. Oshiro G, Owens JC, Shellman Y, Sclafani RA, Li JJ. Cell cycle control of Cdc7p kinase activity through regulation of Dbf4p stability. Mol Cell Biol 1999; 19:4888-96.

36. Kumagai H, Sato N, Yamada M, Mahony D, Seghezzi W, Lees E, et al. A novel growth- and cell cycle-regulated protein, ASK, activates human Cdc7-related kinase and is essential for G1/S transition in mammalian cells. Mol Cell Biol 1999; 19:5083-95.

37. Ferreira MF, Santocanale C, Drury LS, Diffley JF. Dbf4p, an essential S phase-promoting factor, is targeted for degradation by the anaphase-promoting complex. Mol Cell Biol 2000; 20:242-8.

618 38. Mantiero D, Mackenzie A, Donaldson A, Zegerman P. Limiting replication initiation factors
619 execute the temporal programme of origin firing in budding yeast. EMBO J 2011; 30:4805-
620 14.

621 39. Kim JM, Nakao K, Nakamura K, Saito I, Katsuki M, Arai K, et al. Inactivation of Cdc7 kinase
622 in mouse ES cells results in S-phase arrest and p53-dependent cell death. EMBO J 2002;
623 21:2168-79.

624 40. Yamashita N, Kim JM, Koiwai O, Arai K, Masai H. Functional analyses of mouse ASK, an
625 activation subunit for Cdc7 kinase, using conditional ASK knockout ES cells. Genes Cells
626 2005; 10:551-63.

627 41. Dickinson ME, Flenniken AM, Ji X, Teboul L, Wong MD, White JK, et al. High-throughput
628 discovery of novel developmental phenotypes. Nature 2016; 537:508-14.

629 42. Suski JM, Ratnayeke N, Braun M, Zhang T, Strmiska V, Michowski W, et al. CDC7-
630 independent G1/S transition revealed by targeted protein degradation. Nature 2022;
631 605:357-65.

632 43. Van Eyck L, De Somer L, Pombal D, Bornschein S, Frans G, Humblet-Baron S, et al. Brief
633 Report: IFIH1 Mutation Causes Systemic Lupus Erythematosus With Selective IgA
634 Deficiency. Arthritis Rheumatol 2015; 67:1592-7.

635 44. Van Nieuwenhove E, Barber JS, Neumann J, Smeets E, Willemsen M, Pasciuto E, et al.
636 Defective Sec61α1 underlies a novel cause of autosomal dominant severe congenital
637 neutropenia. J Allergy Clin Immunol 2020; 146:1180-93.

638 45. Van Nieuwenhove E, Garcia-Perez JE, Helsen C, Rodriguez PD, van Schouwenburg PA,
639 Dooley J, et al. A kindred with mutant IKAROS and autoimmunity. J Allergy Clin Immunol
640 2018; 142:699-702.e12.

641 46. Staels F, Lorenzetti F, De Keukeleere K, Willemsen M, Gerbaux M, Neumann J, et al. A
642 Novel Homozygous Stop Mutation in IL23R Causes Mendelian Susceptibility to
643 Mycobacterial Disease. J Clin Immunol 2022; 42:1638-52.

644 47. Gupta D, Shah HP, Malu K, Berliner N, Gaines P. Differentiation and characterization of
645 myeloid cells. Curr Protoc Immunol 2014; 104:22f.5.1-f.5.8.

646 48. Sim NL, Kumar P, Hu J, Henikoff S, Schneider G, Ng PC. SIFT web server: predicting
647 effects of amino acid substitutions on proteins. Nucleic Acids Res 2012; 40:W452-7.

648 49. Adzhubei IA, Schmidt S, Peshkin L, Ramensky VE, Gerasimova A, Bork P, et al. A method
649 and server for predicting damaging missense mutations. Nat Methods 2010; 7:248-9.

650 50. Kircher M, Witten DM, Jain P, O'Roak BJ, Cooper GM, Shendure J. A general framework
651 for estimating the relative pathogenicity of human genetic variants. Nat Genet 2014;
652 46:310-5.

653 51. Itan Y, Shang L, Boisson B, Ciancanelli MJ, Markle JG, Martinez-Barricarte R, et al. The
654 mutation significance cutoff: gene-level thresholds for variant predictions. Nat Methods
655 2016; 13:109-10.

656 52. Hughes S, Elustondo F, Di Fonzo A, Leroux FG, Wong AC, Snijders AP, et al. Crystal
657 structure of human CDC7 kinase in complex with its activator DBF4. Nat Struct Mol Biol
658 2012; 19:1101-7.

659 53. Dick SD, Federico S, Hughes SM, Pye VE, O'Reilly N, Cherepanov P. Structural Basis for
660 the Activation and Target Site Specificity of CDC7 Kinase. Structure 2020; 28:954-62.e4.

661 54. Deng C, Zhang P, Harper JW, Elledge SJ, Leder P. Mice lacking p21CIP1/WAF1 undergo
662 normal development, but are defective in G1 checkpoint control. Cell 1995; 82:675-84.

663 55. Brugarolas J, Chandrasekaran C, Gordon JI, Beach D, Jacks T, Hannon GJ. Radiation-
664 induced cell cycle arrest compromised by p21 deficiency. Nature 1995; 377:552-7.

665 56. Shieh SY, Ikeda M, Taya Y, Prives C. DNA damage-induced phosphorylation of p53
666 alleviates inhibition by MDM2. Cell 1997; 91:325-34.

667 57. Rogakou EP, Pilch DR, Orr AH, Ivanova VS, Bonner WM. DNA double-stranded breaks
668 induce histone H2AX phosphorylation on serine 139. J Biol Chem 1998; 273:5858-68.

669 58. Binz SK, Sheehan AM, Wold MS. Replication protein A phosphorylation and the cellular
670 response to DNA damage. DNA Repair (Amst) 2004; 3:1015-24.

671 59. Zhao H, Piwnica-Worms H. ATR-mediated checkpoint pathways regulate phosphorylation
672 and activation of human Chk1. Mol Cell Biol 2001; 21:4129-39.

673 60. Montagnoli A, Tenca P, Sola F, Carpani D, Brotherton D, Albanese C, et al. Cdc7 inhibition
674 reveals a p53-dependent replication checkpoint that is defective in cancer cells. Cancer
675 Res 2004; 64:7110-6.

676 61. Montagnoli A, Valsasina B, Croci V, Menichincheri M, Rainoldi S, Marchesi V, et al. A Cdc7
677 kinase inhibitor restricts initiation of DNA replication and has antitumor activity. Nat Chem
678 Biol 2008; 4:357-65.

679 62. Tudzarova S, Trotter MW, Wollenschlaeger A, Mulvey C, Godovac-Zimmermann J,
680 Williams GH, et al. Molecular architecture of the DNA replication origin activation
681 checkpoint. EMBO J 2010; 29:3381-94.

682 63. Pomerantz J, Schreiber-Agus N, Liégeois NJ, Silverman A, Alland L, Chin L, et al. The
683 Ink4a tumor suppressor gene product, p19Arf, interacts with MDM2 and neutralizes
684 MDM2's inhibition of p53. Cell 1998; 92:713-23.

685 64. Zhang Y, Xiong Y, Yarbrough WG. ARF promotes MDM2 degradation and stabilizes p53:
686 ARF-INK4a locus deletion impairs both the Rb and p53 tumor suppression pathways. Cell
687 1998; 92:725-34.

688 65. Iwai K, Nambu T, Dairiki R, Ohori M, Yu J, Burke K, et al. Molecular mechanism and
689 potential target indication of TAK-931, a novel CDC7-selective inhibitor. Sci Adv 2019;
690 5:eaav3660.

691 66. Mora-Jensen H, Jendholm J, Fossum A, Porse B, Borregaard N, Theilgaard-Mönch K.
692 Technical advance: immunophenotypical characterization of human neutrophil
693 differentiation. J Leukoc Biol 2011; 90:629-34.

694 67. Grassi L, Pourfarzad F, Ullrich S, Merkel A, Were F, Carrillo-de-Santa-Pau E, et al.
695 Dynamics of Transcription Regulation in Human Bone Marrow Myeloid Differentiation to
696 Mature Blood Neutrophils. Cell Rep 2018; 24:2784-94.

697 68. Tsuji T, Ficarro SB, Jiang W. Essential role of phosphorylation of MCM2 by Cdc7/Dbf4 in
698 the initiation of DNA replication in mammalian cells. Mol Biol Cell 2006; 17:4459-72.

699 69. Thakur BL, Baris AM, Fu H, Redon CE, Pongor LS, Mosavarpour S, et al. Convergence of
700 SIRT1 and ATR signaling to modulate replication origin dormancy. Nucleic Acids Res
701 2022; 50:5111-28.

702 70. Barlow JL, Drynan LF, Hewett DR, Holmes LR, Lorenzo-Abalde S, Lane AL, et al. A p53-
703 dependent mechanism underlies macrocytic anemia in a mouse model of human 5q-
704 syndrome. Nat Med 2010; 16:59-66.

705 71. Bellanné-Chantelot C, Schmaltz-Panneau B, Marty C, Fenneteau O, Callebaut I, Clauin S,
706 et al. Mutations in the SRP54 gene cause severe congenital neutropenia as well as
707 Shwachman-Diamond-like syndrome. Blood 2018; 132:1318-31.

708 72. Ceccaldi R, Parmar K, Mouly E, Delord M, Kim JM, Regairaz M, et al. Bone marrow failure
709 in Fanconi anemia is triggered by an exacerbated p53/p21 DNA damage response that
710 impairs hematopoietic stem and progenitor cells. Cell Stem Cell 2012; 11:36-49.

711 73. Dutt S, Narla A, Lin K, Mullally A, Abayasekara N, Megerdichian C, et al. Haploinsufficiency
712 for ribosomal protein genes causes selective activation of p53 in human erythroid
713 progenitor cells. Blood 2011; 117:2567-76.

714 74. Fok WC, Niero ELO, Dege C, Brenner KA, Sturgeon CM, Batista LFZ. p53 Mediates
715 Failure of Human Definitive Hematopoiesis in Dyskeratosis Congenita. Stem Cell Reports
716 2017; 9:409-18.

717 75. Zambetti NA, Bindels EM, Van Strien PM, Valkhof MG, Adisty MN, Hoogenboezem RM,
718 et al. Deficiency of the ribosome biogenesis gene Sbds in hematopoietic stem and
719 progenitor cells causes neutropenia in mice by attenuating lineage progression in
720 myelocytes. Haematologica 2015; 100:1285-93.

721 76. Toki T, Yoshida K, Wang R, Nakamura S, Maekawa T, Goi K, et al. De Novo Mutations
722 Activating Germline TP53 in an Inherited Bone-Marrow-Failure Syndrome. Am J Hum
723 Genet 2018; 103:440-7.

724 77. Toufektchan E, Lejour V, Durand R, Giri N, Draskovic I, Bardot B, et al. Germline mutation
725 of MDM4, a major p53 regulator, in a familial syndrome of defective telomere maintenance.
726 Sci Adv 2020; 6:eaay3511.

727 78. Calnan DR, Brunet A. The FoxO code. Oncogene 2008; 27:2276-88.

728 79. Skokowa J, Lan D, Thakur BK, Wang F, Gupta K, Cario G, et al. NAMPT is essential for
729 the G-CSF-induced myeloid differentiation via a NAD(+)-sirtuin-1-dependent pathway. Nat
730 Med 2009; 15:151-8.

731 80. Vaziri H, Dessain SK, Ng Eaton E, Imai SI, Frye RA, Pandita TK, et al. hSIR2(SIRT1)
732 functions as an NAD-dependent p53 deacetylase. Cell 2001; 107:149-59.

733 81. Dannenmann B, Zahabi A, Mir P, Oswald B, Bernhard R, Klimiankou M, et al. Human
734 iPSC-based model of severe congenital neutropenia reveals elevated UPR and DNA
735 damage in CD34(+) cells preceding leukemic transformation. Exp Hematol 2019; 71:51-
736 60.

737 82. Xu Y, Nasri M, Dannenmann B, Mir P, Zahabi A, Welte K, et al. NAMPT/SIRT2-mediated
738 inhibition of the p53-p21 signaling pathway is indispensable for maintenance and
739 hematopoietic differentiation of human iPS cells. Stem Cell Res Ther 2021; 12:112.

740 83. Deordieva E, Shvets O, Voronin K, Maschan A, Welte K, Skokowa J, et al. Nicotinamide
741 (vitamin B3) treatment improves response to G-CSF in severe congenital neutropenia
742 patients. Br J Haematol 2021; 192:788-92.

743

744 **FIGURE LEGENDS**

745

746 **Fig 1 Homozygous hypomorphic *DBF4* mutation in a patient with syndromic severe**
747 **congenital neutropenia. A**, Schematic representation of the kindred. **B**, Hematoxylin and
748 eosin stain of a bone marrow core biopsy taken at age 19 years after withdrawing G-CSF
749 treatment for two days. Normocellular bone marrow with a prominent paratrabecular cuff of
750 immature myeloid cells without maturation towards the central intertrabecular zone. Virtually
751 no band or segmented neutrophils are observed. Bone marrow eosinophilia is present.
752 Magnification 40x, scale bar 50 µm. **C**, Absolute neutrophil counts during follow-up. Horizontal
753 dashed lines indicate upper and lower reference value. **D**, Sanger chromatograms showing
754 sequencing results of the *DBF4* variant identified in the kindred. **E**, Protein alignment of DBF4
755 orthologs showing conservation of relevant residues across species. **F**, CADD score versus
756 mean allelic frequency (MAF) for the K209N DBF4 variant as compared to homozygous DBF4
757 variants reported in the gnomAD v2.1.1 database. **G**, Domain structure of the DBF4 protein.
758 **H**, Co-immunoprecipitation of endogenous CDC7 with FLAG-tagged WT and mutant DBF4 in
759 HEK293T cells A representative Western blot is shown. **I**, Quantification of three independent
760 co-immunoprecipitation experiments. Values are represented as mean +/- SD. Unpaired two-
761 sided T test.

762

763 **Fig 2 Impaired S phase entry and proliferation in patient T cells. A**, Cell cycle analysis of
764 72 hours stimulated T cells. **B**, Quantification of percentage of T cells in different cell cycle
765 phases after 72 hours of stimulation (n=4 biological replicates). **C**, Proliferation dye dilution
766 assay in T cells stimulated for the indicated time. **D**, Quantification of T cell proliferation after
767 stimulation for the indicated time (n=3 biological replicates). **E**, Western blot showing protein
768 expression in 72 hour stimulated T cells (n=2 biological replicates). The upper target band in
769 the S40/41-MCM2 blot is marked by an asterisk, the lower band is unspecific (See Fig E3 in
770 the Online Repository). **F**, Apoptosis assay in 72 hour stimulated T cells. **G**, Quantification of

apoptotic $CD8^+$ T cells after 72 hours of stimulation (n=3 biological replicates). Values are represented as mean +/- SD. Unpaired two-sided T test.

Fig 3 Perturbed S phase entry and progression, and heightened sensitivity to DDK inhibition in patient fibroblasts. A, Western blot showing protein expression in exponentially-growing passage 8 dermal fibroblasts (n= 2 biological replicates). Uncropped blot and quantification are shown in Fig E5 in the Online Repository. The upper target band in the S40/41-MCM2 blot is marked by an asterisk, the lower band is unspecific (See Fig E3 in the Online Repository). **B**, Cell cycle analysis of serum-starved fibroblasts released into the cell cycle for the indicated time. **C**, Quantification of the percentage of fibroblasts in different cell cycle phases 18 hours after release from serum starvation (n=3 biological replicates). **D**, Single cell cycle progression assay of serum-starved fibroblasts released into the cell cycle in the presence of nocodazole +/- TAK-931. **E**, Quantification of the percentage of fibroblasts in G2/M after release from serum starvation in the presence of nocodazole for the indicated time (n=4 biological replicates). **F**, Quantification of fibroblasts in G2/M 48 hours after release from serum starvation in the presence of EdU, nocodazole and TAK-931 as a percentage of fibroblasts released without TAK-931 (n=4 biological replicates). **G**, Quantification of the percentage of fibroblasts in S phase 48 hours after release from serum starvation in the presence of EdU, nocodazole and TAK-931 (n=4 biological replicates). Values are represented as mean +/- SD. Unpaired two-sided T test.

Fig 4. p53-p21 pathway activation impairs neutrophil differentiation. A, Promyelocytic HL60 cells differentiation assay in the presence or absence of TAK-931. HL60 cells were differentiated for 6 days in the presence of DMSO. B, Quantification of the percentage of promyelocyte-like and metamyelocyte/neutrophil-like HL60 cells after 6 days of differentiation (n=4 biological replicates). **C**, Granulocytic differentiation of peripheral blood $CD34^+$ cells for 13 days. Patient $CD34^+$ cells were transduced with lentivirus encoding GFP or WT DBF4. **D**,

798 Quantification of the percentage of promyelocytes, myelocytes and
799 metamyelocytes/neutrophils after 13 days of granulocytic differentiation (n=2 biological
800 replicates for untransduced conditions, n=1 experiment for transduced conditions). **E**,
801 *CDKN1A* gene expression analysis of day 16 differentiated $CD34^+$ cells and peripheral blood
802 (PB) and bone marrow (BM) *ex vivo* granulocytes (n=2 technical replicates). **F**, Western blot
803 showing p53 protein expression in *ex vivo* granulocytes (n=1 experiment). Values are
804 represented as mean +/- SD. One-way ANOVA with correction for multiple comparisons.

Figure 1

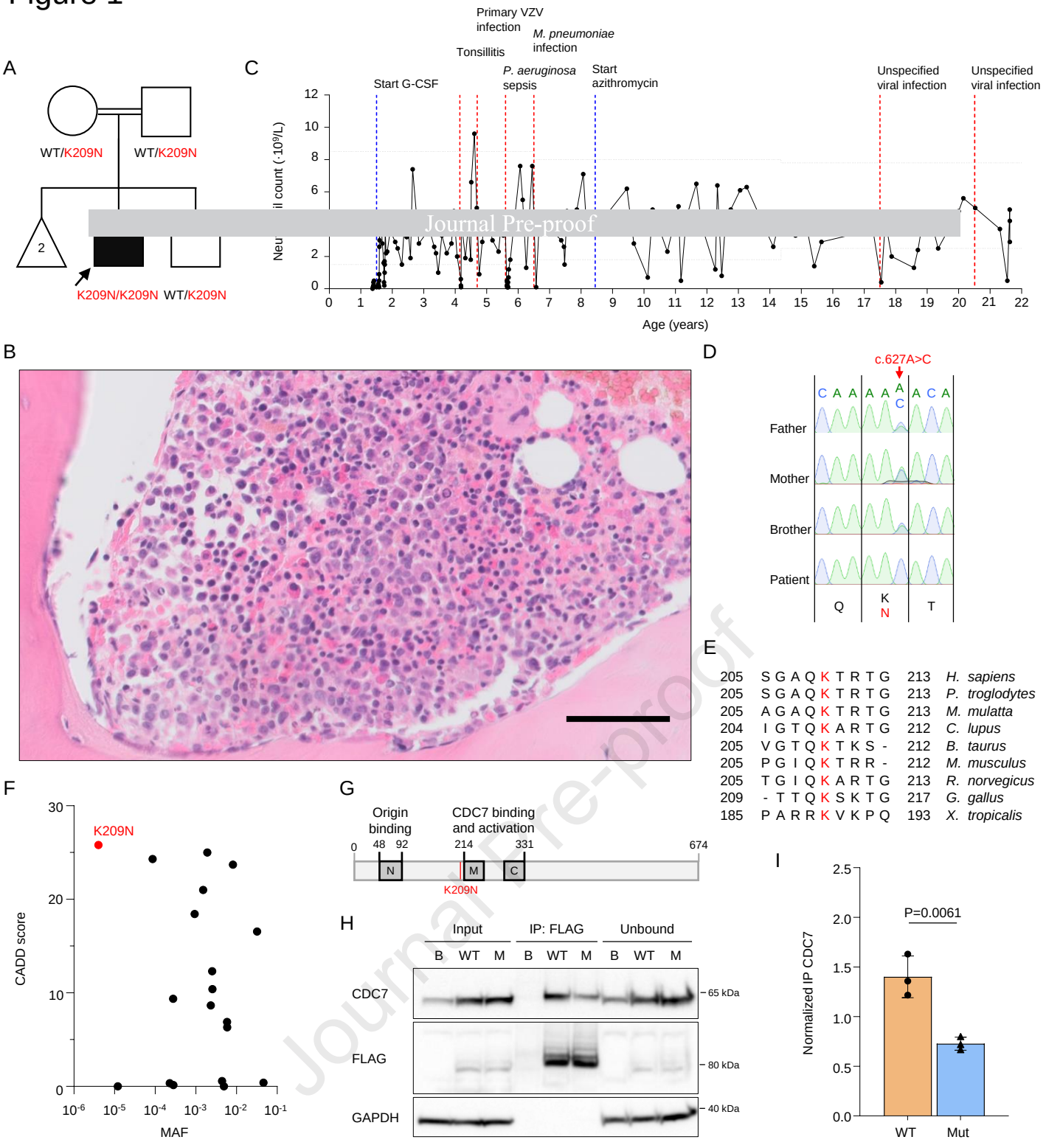

Figure 2

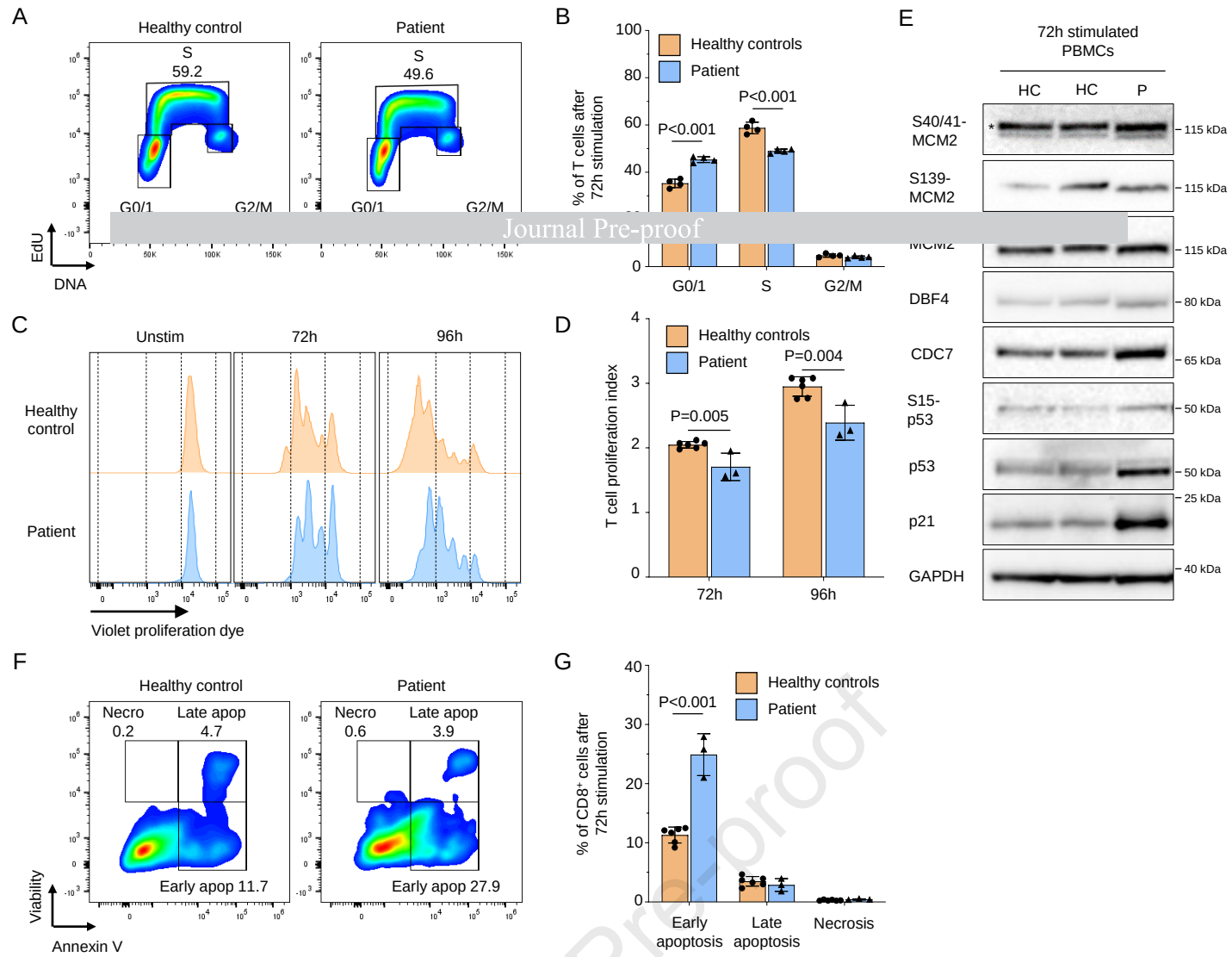

Figure 3

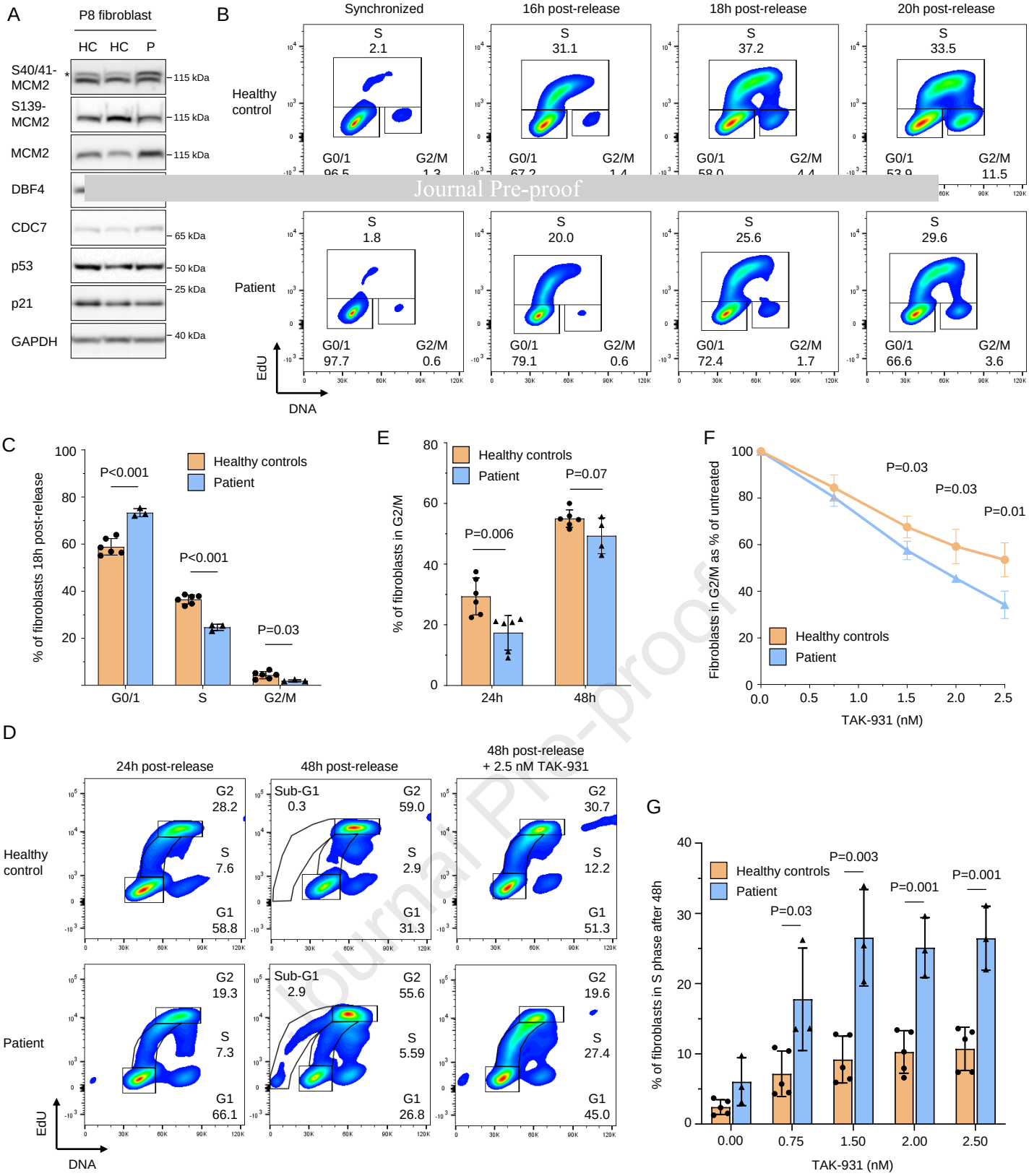

Figure 4